FACTA UNIVERSITATIS
Series: **Mechanical Engineering**
https://doi.org/10.22190/FUME240801041A

Original scientific paper

A COMPARATIVE STUDY ON MECHANICAL PERFORMANCE OF PLA, ABS, AND CF MATERIALS FABRICATED BY FUSED DEPOSITION MODELING

Cem Alparslan[1], Şenol Bayraktar[1], Kapil Gupta[2]

[1]Mechanical Engineering, Faculty of Engineering and Architecture,
Recep Tayyip Erdoğan University, Rize, Türkiye
[2]Mechanical and Industrial Engineering Technology, University of Johannesburg,
Johannesburg, South Africa

Abstract. *Fused deposition modeling (FDM) is one of the most extensively used additive manufacturing (AM) techniques. This study contributes to the knowledge enhancement related to AM by presenting the details of experimental investigation conducted on FDM of three different materials i.e. polylactic acid (PLA), acrylonitrile butadiene styrene (ABS) and carbon fiber (ePA-CF) and providing the common optimum fabrication parameters for FDM of PLA, ABS and ePA-Cf materials. A detailed analysis of the effect of two important FDM parameters, namely infill pattern (IP) and layer thickness (LT), on mechanical properties of the fabricated samples from the materials, has been done. The best mechanical properties of the PLA sample were obtained with LT of 0.15 mm and hexagon pattern, of the ABS sample were obtained with LT of 0.15 mm and triangle pattern, and of the ePA- CF sample were observed at LT of 0.15 mm and hexagon pattern. It was determined that elongation, yield (YS) and tensile strength (TS) decreased with increasing LT in all materials' samples. While the fracture surfaces of PLA samples were smooth, and the layer lines were evident. Whereas the fracture surfaces of ABS samples were rough, and the lines were less distinct than PLA. On the other side, the fracture surfaces in ePA-CF samples had a fibrous structure. The voids formed between layers were seen the most in PLA and the least in ePA-CF samples. LT of 0.15 mm and hexagon IP. It was observed that the best results in terms of mechanical properties were obtained under LT of 0.15 mm and IP of hexagon conditions.*

Key words: *Additive manufacturing, Fracture, Mechanical properties, FDM, PLA, Rapid prototyping*

Received: August 01, 2024 / Accepted September 25, 2024
Corresponding author: Şenol Bayraktar
Mechanical Engineering, Faculty of Engineering and Architecture, Recep Tayyip Erdoğan University, Rize, Türkiye
E-mail: senol.bayraktar@erdogan.edu.tr

1. INTRODUCTION

In recent times, there has been a growing interest in technologies related to AM. AM technologies are becoming a promising alternative to traditional production methods such as machining, casting, and injection molding, because of their significant benefits such as suitability for mass production, affordability, customization, and quick prototyping [1-3]. The most frequently utilized AM techniques are FDM and selective laser sintering (SLS). These methods offer remarkable advantages over traditional manufacturing techniques [4-8]. These advantages include properties such as low initial costs, material diversity, fast manufacture processes and the ability to easily produce complex parts [9-11]. Parts manufactured with these methods do not necessarily additional surface engineering processes such as heat treatment, chemical surface modification or mechanical processing. FDM and SLS are ideal for applications in sectors like medical, aviation and automotive, by enabling the manufacture of lightweight, high-strength and customized parts [12-15]. Additionally, FDM technology allows for the production of parts without geometric limitations and removes the necessity for milling or other post-processing steps commonly required in most metal-based 3D printing technologies. In this way, it makes it possible to reduce or eliminate stress in the produced material. FDM is emerging as a technology used in the production of workpieces with dimensional accuracy, repeatability and high strength. Lighter and three-dimensional complex geometries can be easily obtained with the effect of design freedom. For this reason, it is used in the production of prototypes for components used in the aviation, military and automotive sectors before the final product. As a result, faulty product costs are minimized in industrial businesses and the chances of businesses competing in the global market increase. FDM, also referred to as filament freeform fabrication (FFF), involves extruding plastic workpiece through heated print equipment. Components are built with continuously layering molten thermoplastic workpiece. Depending on the geometric structures, additional support structures may be required. Initially utilized for creating low-cost prototypes and concept models, this method is now favored for producing high-quality functional prototypes and concept models [16, 17]. The most used materials for FDM 3D printing include ABS, Polycarbonates (PC), Acrylonitrile Styrene Acrylate (ASA), and PLA. With the developments in material science, the materials used in the FDM method are constantly changing. The integration of carbon fiber, graphene, and other composite materials importantly develops mechanical properties of parts manufactured with FDM, making them more durable, lightweight, and functional. Such developments are shaping the future of AM technologies, providing access to wider application areas and industrial sectors [18]. PLA turns into harmless lactic acid over time [19]. Therefore, it is immunologically inactive [20]. It is preferred for use in the medical implant (screw and pin) sector due to this feature. ABS is becoming attractive in the industry to produce demanding consumer products due to its excellent impact and mechanical strength, dimensional stability and electrical insulation properties. Therefore, it provides significant advantages in the production of safety helmets, automotive dashboards and other interior components, pipe fittings, home security devices and small household appliances and communication equipment [21]. PA-CF composites are used in the production of equipment such as automotive brackets, inspection gauges, robotic end effectors, and under-hood applications in the automotive industry. In addition, the use of these materials in the industry can contribute to cost reductions and improved operational efficiency [22].

We have reviewed some previous studies conducted on fabrication of various parts and components using FDM method. Yu et al. created specimens using the FDM method by blending PLA and PBS (Polybutylene Succinate) filaments together [23]. They examined the effect of PBS addition on PLA filaments with these samples. They concluded that among PBS/PLA mixtures, 10% PBS/PLA is an ideal mixture for biodegradable raw material. Sedlacek and Lasova [24] investigated the effect of short carbon fibers on the nylon PA6 polymer used in the FDM process. They examined the mechanical properties of samples printed horizontally and vertically with the FDM method. They found that short CFs significantly affected force (12%) and heat resistance of PA6 components. Comparing the longitudinal reinforcement of fibres in PA6 with the transverse reinforcement, they determined a 39% increase in strength and tensile modulus. Farashi et al. [25] conducted a meta-analysis study to investigate the effect of the PS and extruder temperature used in the FDM method on the tensile strength of the produced samples. They carried out their search strategies using appropriate search terms and statistical calculation methods. As a result of the study, it was seen that rising extruder temperature had favorable impact on tensile strength (Standard mean difference= 2.85, 95% Confidence interval [1.71, 3.98]), while increasing printing speed had a negative effect (SMD= - 2.49, 95% CI [-4.29, -0.69]). Bochnia et al. [26] researched mechanical features of FDM parts obtained from PLA and PLA-CF reinforced materials in terms of thin-walled practices. In their studies, samples with different thicknesses (1, 1.4 and 1.8 mm) and printing orientations (X, Y and Z) were subjected to tensile testing for two materials. They determined that CF-reinforced PLA samples had superior strength than samples made of pure PLA. Additionally, they observed a 40% lower tensile strength in the Z (vertical) direction compared to other sample types. Chalgham et al. [27] examined mechanical features of PLA parts manufactured by FDM method before and after heat treatment. Three-point bending tests were conducted to assess the effect of parameters like layer thickness (LT), printing temperature (PT), and PS on the mechanical properties. They found that the optimum parameters were in the X-Z printing direction, spraying temperature of 190 ^{o}C, PS of 90 mm/s and LT of 0.3 mm. They stated that the maximum force during bending increased by 2% as a result of subjecting the samples produced with optimum parameters to 75 ^{o}C thermal post-treatment. Samykano et al. [28] conducted the effect of three different manufacture parameters such as layer height, scanning angle and filling density on the mechanical properties of ABS samples in the FDM method. They found that the optimum production parameters were filling rate of 80%, LT of 0.5 mm and scanning angle of 65^{o}. They developed a mathematical equation using surface response methodology (R^2: 85.80%) to numerically predict the tensile features of ABS workpiece and determine optimum production parameters. Khabia et al. [29] studied a comparative study on the mechanical features of components produced with three different FDM printers (Accucraft i250, Arya UNO+, and Zortrax M200) using ABS filament material combinations (Low-cost ABS filament and Z-ABS). They tested tensile parts according to ASTM D 638 standard on a 3382 electromechanical universal testing system. They determined that the sample exhibiting the best mechanical properties (Z-ABS filament material) was according to the production parameters found in the Ultimaker Cura 3.6 slicing software. Pazhamannil et al. [30] evaluated the effect of production parameters like filling ratio, infill pattern (IP), extruder temperature, LT, PS and heat treatment processes on mechanical features of PLA and CF-PLA components prepared by the FDM method. They determined that the maximum mechanical properties of both filaments occurred at PS of 30 mm/s and infill rate of 90% for the gyroid pattern with layer height of

0.1 mm. They found that tensile properties of CF reinforced tensile samples were higher than those of standard polylactic acid. Additionally, after an annealing process at 95°C for 60 minutes, they observed a 14.01% increase in the maximum stresses of PLA-CF materials. Reverte et al. [31] analyzed the mechanical and geometric properties of PLA and PLA-CF components prepared with FFF technique. They carried out tensile, bending and ILSS (Inter laminar shear strength) tests to obtain mechanical performance of dissimilar specimens. They observed that addition of CFs enhanced the mechanical characteristics of PLA-CF composites compared to pure PLA. Dhinesh et al. [32] investigated different types of raw materials (PLA and ABS combination) to provide better mechanical features of parts manufactured using AM technology. In their study, they produced samples with various compositions using the FDM method in order to present a new filament that could withstand higher tensions than traditional filaments. These different compositions (20% ABS and 80% PLA; 50% ABS and 50% PLA; 50% ABS and 50% PLA; 50% ABS and 50% PLA; 20% ABS and 80% PLA; 80% ABS and 20% PLA) were researched for their resistance to tensile and bending loads. As a result of the study, they found that the ABS and PLA sandwiching concept exhibited better mechanical properties. AM technologies, despite bringing significant innovations to production processes, cannot ignore the challenges and limitations they face. Factors such as the properties of materials used in the manufacturing process, printing techniques, and surface quality can directly impact the performance of the final products. Anisotropy occurring during the printing process can lead to inconsistencies in the mechanical properties of manufactured parts, which can limit their use in industrial applications. In this context, research and development are focused on advancing AM technologies, overcoming these challenges and further improving processes. In the future, with the evolution of AM technologies and the exploration of new material combinations, it is expected that this technology will have the capacity to revolutionize industrial manufacture more broadly. In addition, AM offers significant advantages in issues such as sustainable production and reduction of environmental impacts. By reducing material waste and increasing energy efficiency, AM is poised to play a key role in sustainable manufacturing solutions. With these features, AM technologies will continue to have a central position in the manufacturing paradigms of the future.

With an aim to contribute to the knowledge base and to develop a deeper understanding of the FDM of different materials, the present research work investigates the effects of different infill patterns (Hexagon, triangle and line) and layer thickness (0.15, 0.25 and 0.35) on the mechanical properties of parts made of PLA, ABS and ePA- CF filaments and fabricated by FDM method. Different types of filament materials, as mentioned above, were chosen because they are widely used in industry and can provide the required mechanical properties suitable for a wide range of applications. In this study, we also developed the understanding of critical parameters to optimize the performance of components produced with FDM and to determine common production parameters for three different materials.

2. MATERIALS AND METHODS

2.1 Material and 3D Printing System

The experiments were carried out on samples produced using commercially available filaments based on PLA, ABS, and ePA-CF. ePA-CF material consists of a nylon 6/66 copolymer with 20% carbon fiber (eSUN, Inc. China). Mechanical properties of materials supplied by the manufacturer were given in Table 1.

Table 1 Mechanical features of PLA, ABS and ePA-CF [33]

Properties	PLA	ABS	ePA-CF
Specific gravity (g/cm^3)	1.2	1.04	1.24
Tensile strength (MPa)	72	43	140
Elongation (%)	11.8	22	10.61
Print temperature (°C)	210-260	230-270	250-300
Print speed (mm/s)	40-100	40-100	40-100

The materials were supplied as ESUN [34] brand in the filament wound on a 1.75 mm diameter spool. PLA, ABS and ePA-CF samples were produced using the Creator 3 desktop 3D printer manufactured by Flashforge [35]. The Flashforge Creator 3 is equipped with features such as a heated build plate and replaceable nozzles, which enable the use of wide range of workpieces. 3D printing system consists of a heated build plate, an extruder, a temperature control system, a mechanism capable of movement along the XYZ axes, and two heated print heads with various nozzle diameters. Details of these components of the printer are depicted in Fig. 1.

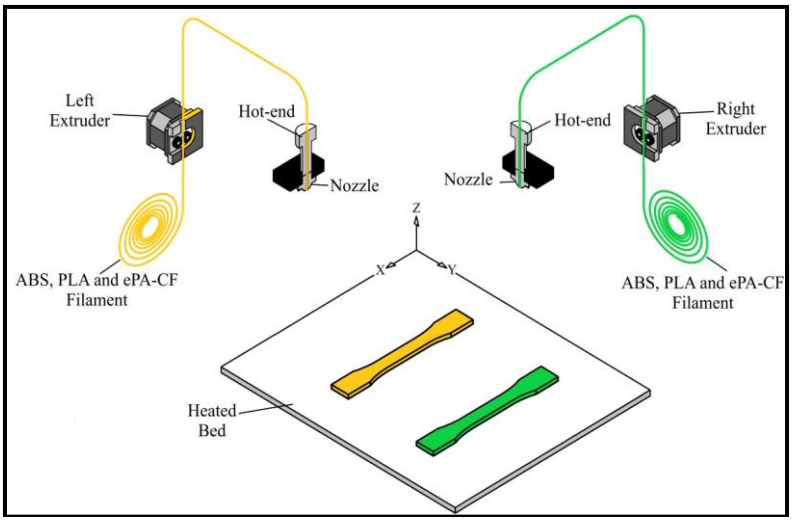

Fig. 1 Schematic representation of built orientation of samples in FDM of ABS, PLA, and ePA-CF

Table 2 Flashforge Creator 3 technical specifications

Parameters	Value
Extruder number	2
Print resolution	± 0.2 mm
Layer resolution	0.05-0.4 mm
Print speed	10-150 mm/s
Maximum extruder temperature	300 C^{o}
Minimum extruder temperature	120 C^{o}

Table 2 displays technical specifications of the Flashforge Creator 3 3D printing equipment. Samples were modeled with CAD software. The modeled files were transferred to the 3D printer as stereolithography files (STL) with good resolution and 0.0171 mm deviation. Flashprint 5 software was utilized to import STL files and generate G-code files compatible with the requirements of the Flashforge Creator 3. This process reveals the 3D printer's ability to work harmoniously with different materials such as PLA, ABS and ePA-CF, and its efficiency in production.

2.2 FDM Machine Settings and Specimen Fabrication

The major aim of the study is to analyze the mechanical impact of different LT'es and IP's on various types of materials. Experimental preliminary studies were conducted, taking into account the information provided by the material manufacturer. In this manner, production was repeated with varying parameters, and choosing of FDM printing settings, which influence geometric and mechanical performance of workpieces produced from ABS, PLA, and ePA-CF samples, was determined collaboratively (Table 3). Tensile test specimens were prepared according to ASTM D638-14 standard Type IV (Fig. 2) [36, 37]. A total of 81 tensile samples were fabricated. The samples were prepared according to three different LT (0.15, 0.25 and 0.35) and IP (Hexagon, triangle and line).

Table 3 FDM process parameters considered in the present work

Parameters	Value
Speed of base (mm/s)	60
Printing speed (mm/s)	80
Height of layer (mm)	0.15, 0.25 and 0.35
Printing temperature (^{o}C)	260
Platform temperature (^{o}C)	100
Nozzle diameter (mm)	0.4
Slice profile	Fine
Infill pattern	Hexagon, triangle and line
Infill density	100%

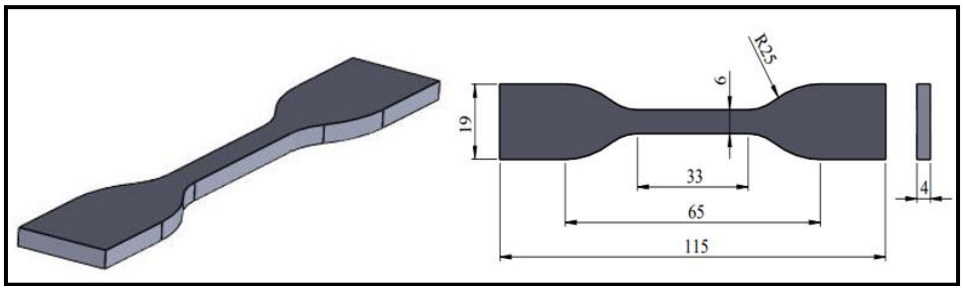

Fig. 2 Dimension and shape of specimens utilized for tensile test (dimensions are in mm)

Irrespective of the 3D printer model in AM technology, it is essential to understand how printing thickness and direction affect the mechanical properties of the constructed models. Thanks to this, it is possible to correlate the test results presented with different types of printers. Fig. 3 shows the variably determined printing parameters.

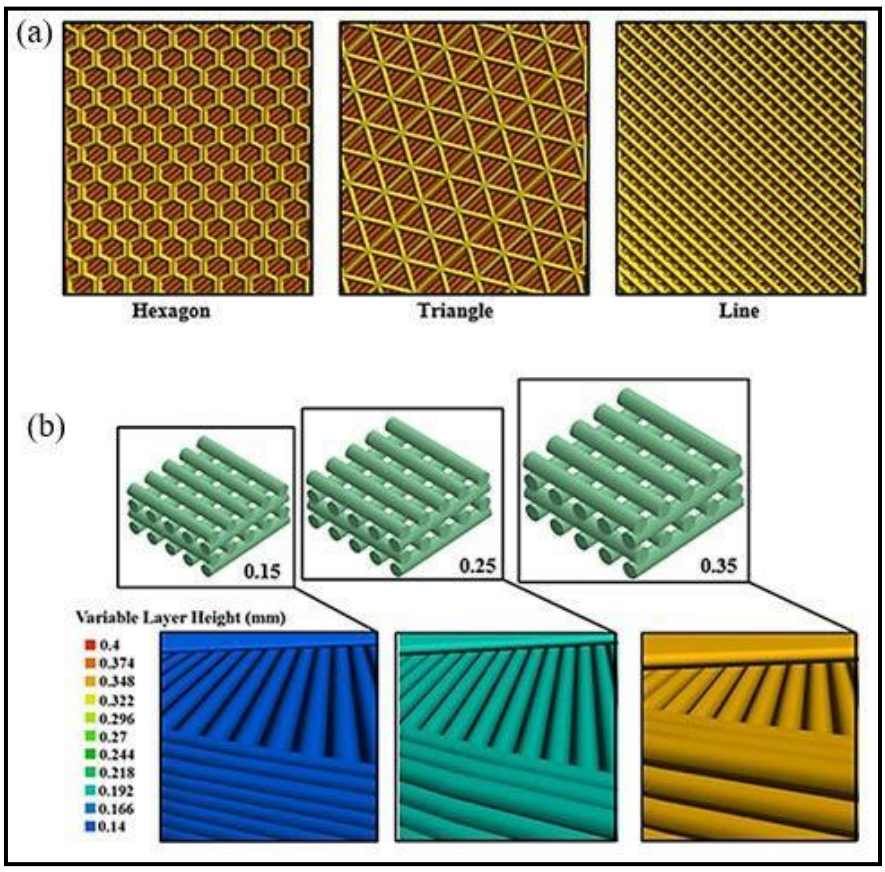

Fig. 3 Process parameters for FDM printed PLA, ABS and ePA-CF specimens, (a) IP types, (b) LT

The tensile samples of the printed examples on the Flashforge Creator 3 FDM printer are given in Fig. 4. Upon completion of the printing process, the support material was detached from the printing plate, and any remaining filaments were removed prior to cleaning the models. The geometries of the samples were re-measured after production to ensure compliance with the ASTM D638-14 Type IV standard. This process is crucial to evaluate whether the produced parts provide the specified features and tolerances. This control stage is of great importance in ensuring the accuracy and production quality of 3D printing, as well as ensuring that the final products exhibit the expected performance in their application areas. Finally, tensile experiments were conducted on samples. As a result of tensile experiments, the test results were determined with the arithmetic average of YS, TS and elongation.

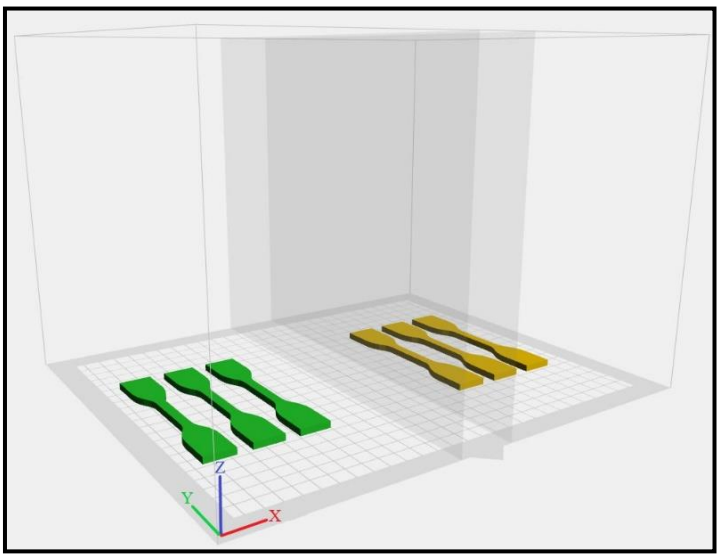

Fig. 4 Arrangement of parts on the printing plate of the Creator 3 print orientation

2.3 Procedure for Mechanical Properties Testing

Tensile tests of PLA, ABS, and ePA-CF specimen were conducted on the Utest-Profi X6 tensile testing device at constant loading rate of 5 mm/min (Fig. 5). Test samples were subjected to tensile tests according to each IP and LT. As a result of the tensile tests, YS (N/mm^2), TS (N/mm^2) and elongation (%) values were obtained. Mechanical tests were carried out by following the EN ISO/IEC 17025 standard. In addition, three samples were produced for each parameter to ensure the reliability of the experimental results in the mechanical tests. The final elongation, yield strength, and tensile strength values were determined by the arithmetic average of the results obtained from these samples. Fractured surfaces were analyzed using Scanning Electron Microscope (SEM). For analysis, all specimens were initially cut to dimensions of 10×5×3 mm and prepared for SEM analysis. To make samples suitable for SEM analysis, conductive coating is often required. In this process, the surface of the specimen was coated with the sputter coater method (Quorum SC7620 machine, 6 minutes, chamber pressure of 200 bar, argon gas and current of 15mA).

This process ensures that the sample becomes conductive under the electron beam, improving image quality and preventing high-energy electrons from damaging the sample.

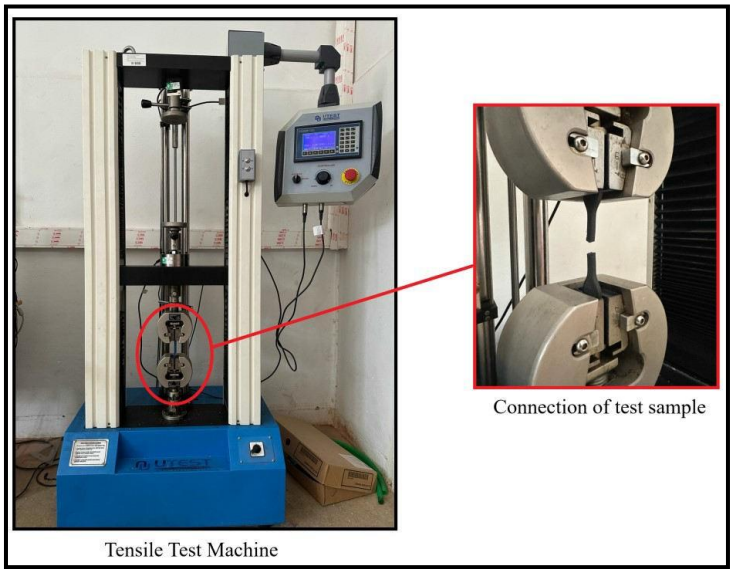

Fig. 5 UTEST PROFI X6 tensile testing machine

3. Results and Discussion

Mechanical features of workpieces produced with FDM technology vary depending on the printing parameters used. These variations are crucial concerning the broad applicability and performance of printed parts. Changes in manufacture parameters can directly affect tensile strength, which is a critical mechanical property that expresses the resistance of a material to tensile force. The main FDM parameters that can be adjusted during printing include layer height, infill density, PS and temperature. Each of these parameters can influence the material's behavior during printing and the microstructure of the final part. These changes in microstructure are reflected in the macroscopic mechanical features of workpiece. Experiments for commonly used FDM filament materials have shown that printing parameters have significant effects on elongation, YS and TS.

3.1 Effect of FDM Variables on Mechanical Features

It was observed that TS and YS decreased in PLA, ABS and ePa-CF samples with increasing LT (Fig. 6). In PLA samples, the highest YS (18.95 MPa) and TS (20.45 MPa) were obtained in the hexagon pattern and LT of 0.15 mm, while the lowest YS value (10.17 MPa) was measured in line pattern and LT of 0.35 mm, and the TS value was (8.48 MPa) in the triangle pattern and LT of 0.35 mm (Fig 6a). In ABS samples, the highest YS (17.11 MPa) was obtained in the hexagon pattern and LT of 0.15 mm, while the highest TS (19.97 MPa) was determined in the triangle pattern and LT of 0.15 mm. The lowest values (TS: 16.90 and YS: 12.52 MPa) were observed in the triangle pattern and LT of 0.35 mm (Fig.

6b). In ePA-CF samples, the highest YS (22.11 MPa) and TS (25.25 MPa) were obtained in the hexagon pattern and LT of 0.15 mm, while the lowest values (TS: 15.96 and YS: 14.53 MPa) were obtained in the line pattern and LT of 0.35 mm (Fig. 6c).

It is well-established that carbon fiber reinforced materials exhibit higher strength, attributed to strength of fibers and bonding between the fibers and the matrix [38]. Additionally, it is thought that as a result of incorporating carbon fibers into the composite material, the load-carrying capacity of the material increases, thus minimizing deformation under load [39]. Moreover, the uniform dispersion (homogeneous) of carbon fibers contributes to an elevated degree of crystallization, effectively preventing localized stress concentrations. Therefore, enhances the material's resistance to fracture [40]. Upon detailed examination during production, it was observed that the accumulation of individually laid fibers layer by layer results in the creation of a layer through integration of polymer bands within, facilitated by the thermal diffusion process. In this context, it was determined that, in addition to interlayer relationships, layers exist adhesion among the accumulated fibers within a specific layer. Changes in the number of structural layers within all materials have been observed to more significantly influence elastic and plastic stress properties as LT increases. This is thought to be due to the combined adhesion force between the intermediate layers.

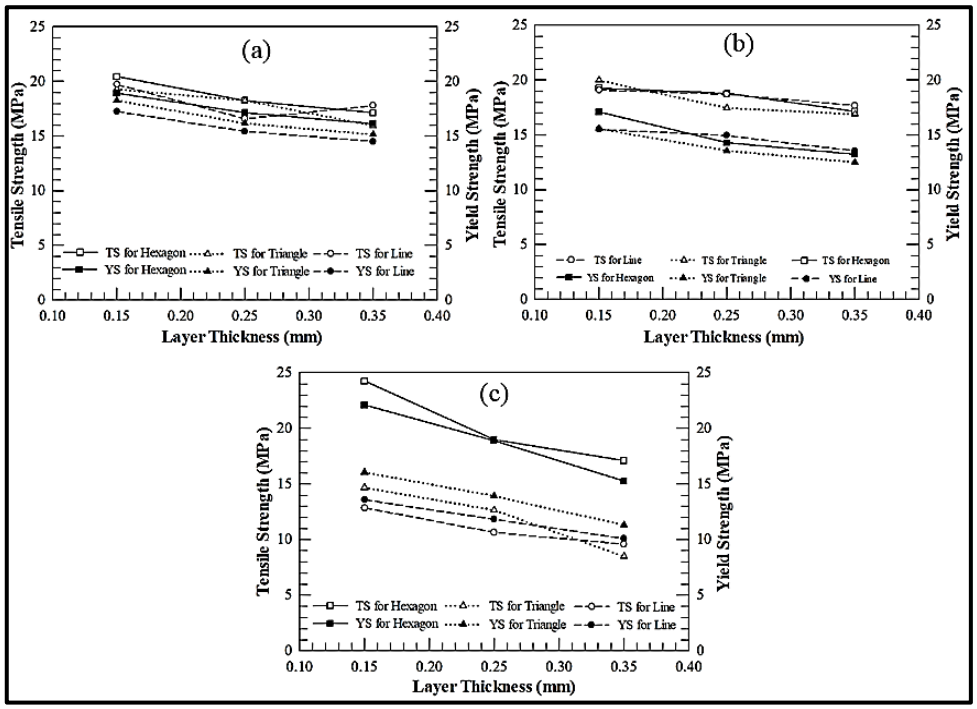

Fig. 6 TS and YS depending on LT, (a) PLA, (b) ABS, (c) ePA-CF

It was observed that with increasing LT in PLA, the elongation decreased by 22.96 (Hexagon), 5.05 (Triangle) and 11.07% (Line) patterns, respectively (Fig. 7a), while it

decreased by 23.64 (Hexagon), 6.35 (Triangle) and 6.96% (Line) patterns for ABS (Fig. 7 b). It was also observed that the ePA-CF material decreased by 30.06 (Hexagon), 32.33 (Triangle) and 33.06% (Line), respectively (Fig. 7c).

The findings revealed that material features were considerably developed by use of certain parameters like LT and IP, with the highest tensile strength values recorded being achieved. However, the effect of LT on elongation, TS and YS cannot be generalized as a linear or one-way relationship. The effect may vary depending on the 3D printing technology used, printing parameters and material properties [41, 42]. When evaluated in general, it was observed that the best results in terms of mechanical properties were obtained under LT of 0.15 mm and IP of hexagon conditions.

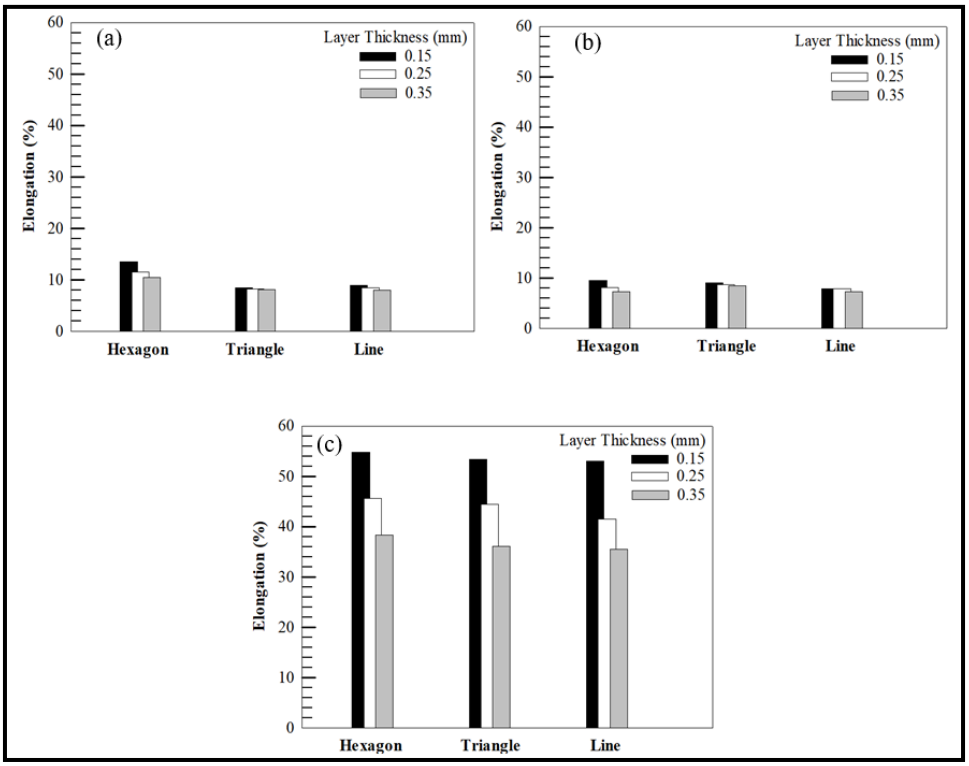

Fig. 7 Elongation depending on LT, (a) PLA, (b) ABS, (c) ePA-CF

3.2 Influence of FDM Parameters on Fracture Surface Characteristics

Regardless of the IP, it was observed that samples with increased LT exhibit behavior closer to a brittle fracture type. SEM images were captured to gather data on impacts of reinforcement elements and structure orientation on morphology of accumulated layers (Fig. 8). In PLA and ABS samples (Fig. 8a and b), it was seen that the flat orientation, where the fracture surface was located on a plane, shows brittle behavior. The cross-sectional shapes of the layers, their periodicity and formation of intrafilamentary voids between the accumulated strips were determined. This is believed to be due to the lower

part of the sample sticking together because of the softened nature of melted filament passing through nozzle during extrusion, while the upper part exhibits a circular, convex structure after cooling [43]. These voids may be the reason for low tensile strength (Fig. 8a and b). Some air voids between layers appear to be more evident for the PLA sample (Fig. 8a).

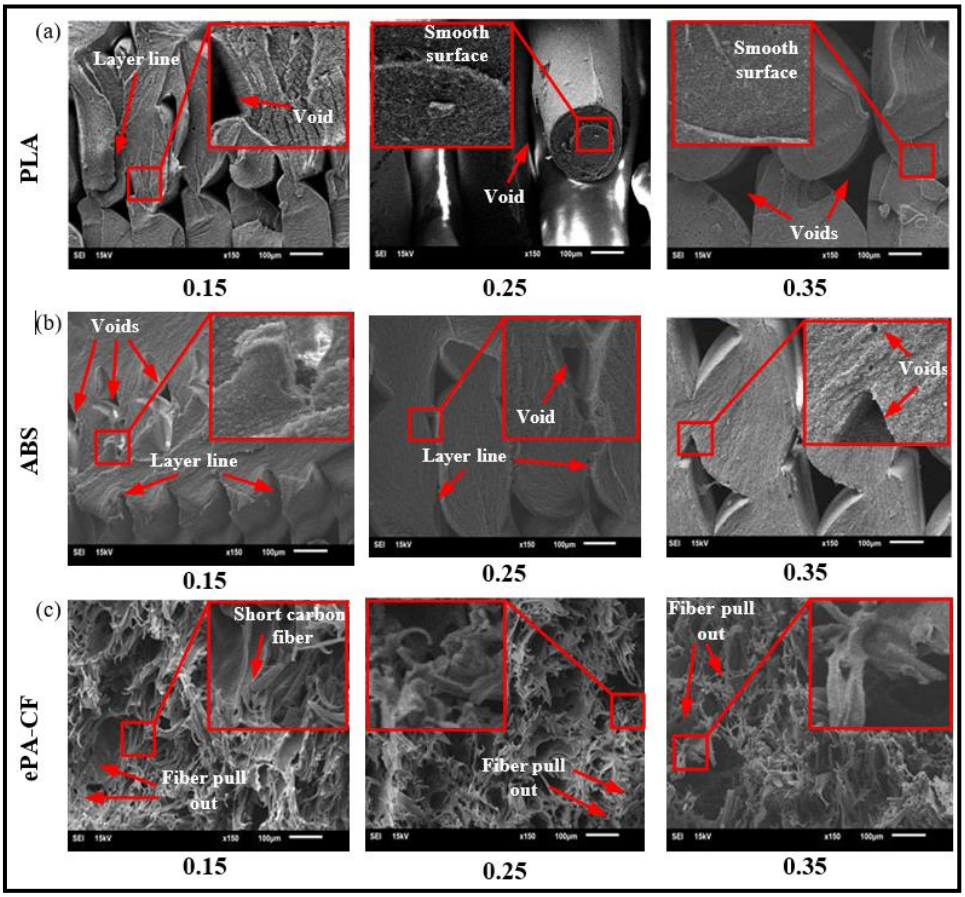

Fig. 8 Fracture surfaces of the examined workpieces, (a) PLA, (b) ABS, (c) ePA-CF

When the PLA material (Fig. 8a), was examined, it was seen that the fracture surface was smooth, and the layer lines were clear. This indicates that the breakage occurs due to interlayer separation caused by insufficient bonding between layers during printing [44-46]. The fracture surface of ABS samples was observed to be rougher and exhibits distinct layer lines compared to PLA samples (Fig. 8b). This is evident that fractures in ABS materials generally occur at the junctions of the layers. Because these regions are weak compared to the general material structure. Furthermore, fracture is thought to occur along the direction in which layers of material are stacked. It shows that this situation is due to the anisotropic structure of ABS materials [47].

Additionally, whitening occurs in ABS materials under strain (Fig. 9). This is a sign that the material has undergone plastic deformation before fracture. During tensile testing, stress whitening may occur, especially in areas close to the breaking point. In most scenarios, fracture of thermoplastic components is characterized by stretching of filamentous macromolecules, allowing a high degree of deformation in the material [48].

This situation is associated with the rearrangement and elongation of the mentioned macromolecules. Moreover, the fracture surfaces of thermoset polymeric components generally do not show significant plastic deformation due to the high degree of cross-linking between their macromolecules. This is thought to occur as a result of cross-links forming a tight bonding between macromolecular chains and thus limiting the plastic flow of the material [49-51].

For the ePA-CF material, carbon fiber reinforcement material is clearly visible on the fractured surfaces (Fig. 8c). This, in addition to high strength and hardness, significantly affects the fracture mechanism of the material [52]. Additionally, directional fractures were observed on the fracture surface for the ePA-CF material. This situation is thought to be due to the material exhibiting anisotropic properties [53-55]. It seems that fiber orientations and lengths are the most effective factors in determining mechanical properties in carbon fiber reinforced materials [56, 57]. In addition, a damage mechanism occurs due to the separation and pulling of fibers from matrix and local deformation occurs in matrix around fibers. When the SEM images were examined in detail, no elongation, wear and characteristic voids near some fibers were observed in the fiber-reinforced matrices. It was found that most of CFs were not aligned in the direction of the print layers, as if they were pieces broken off from longer fibers. No printing layer could be observed in the ePA-CF material. The layers were roughly identified and determined based on orientation of fibers (Fig. 8c). The increase in LT is tough to result in a less homogeneous structure for the ePA-CF material, consequently weakening the connections between layers.

This is proven by the decrease in the tensile strength of the part. It is also thought that thicker layers are more pronounced and may increase the roughness of the fracture surfaces.

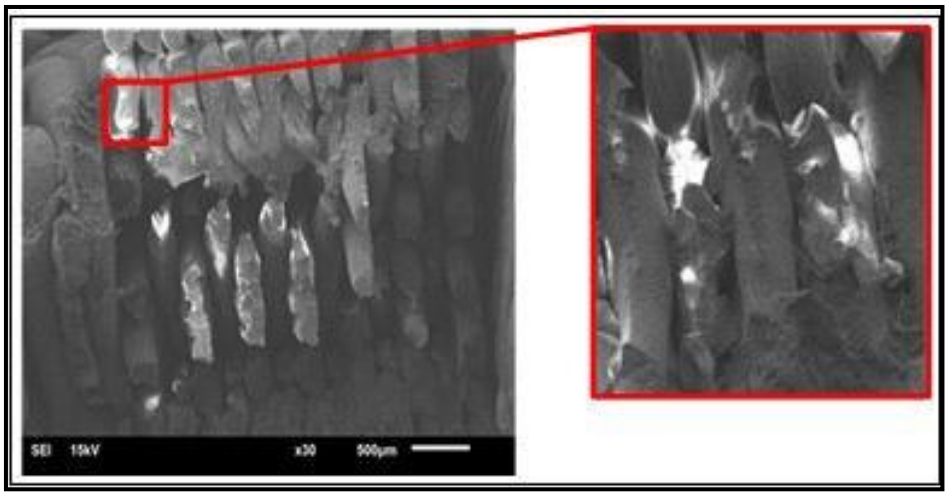

Fig. 9 Fracture surfaces of the ABS specimen

More material deposition is required in all samples produced by increasing the LT. Therefore, a long printing time is required. Longer printing times result in increased thermal effects on the produced samples. This causes thermal stresses in the samples. It is thought that these stresses cause cracks to form on the fracture surfaces and change the fracture behavior of the part.

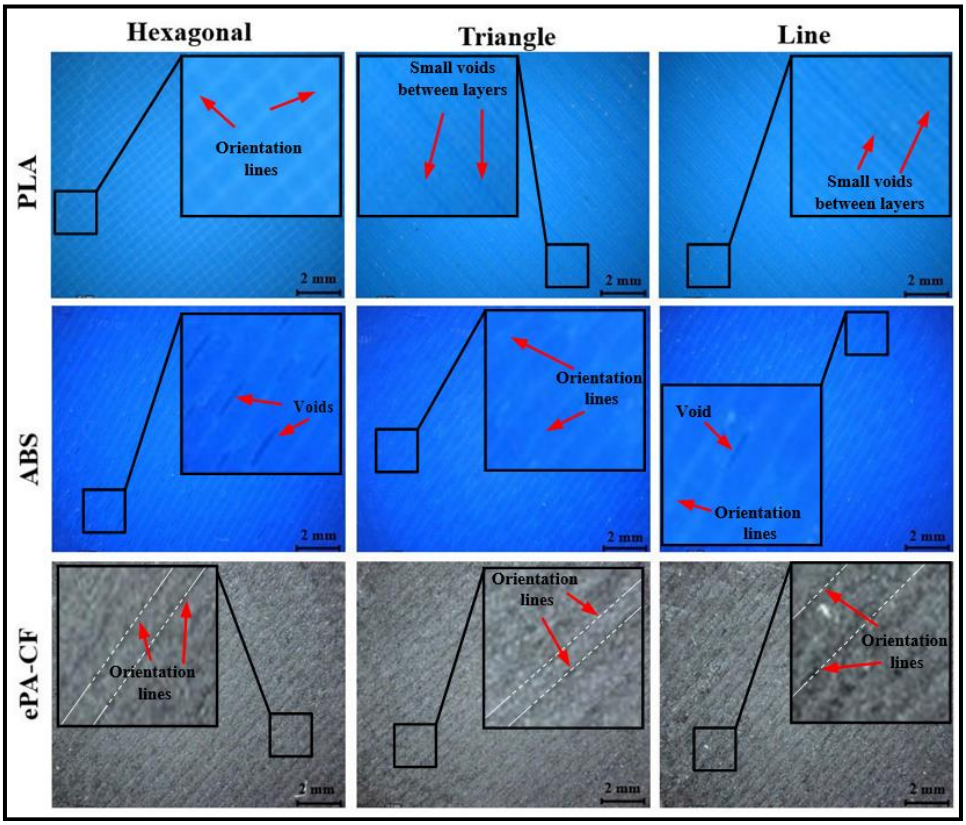

Fig. 10 Microscopic images of the orientations of hexagon, triangle and line patterns

A common defect in FDM manufacturing is the development of internal stresses within the workpiece during printing, which is attributed to the rapid cooling and heating cycles. This situation brings about uneven temperature changes, resulting in the formation of residual stresses. Fast cooling ensures rapid solidification of the accumulated layer. When newly extruded filament is deposited onto solidified layer, a local re-melting impact occurs, facilitating bond formation between the filament and solidified layer [58]. However, as the LT increases, the cooling and solidification rate decreases. This causes uneven heating and cooling of the workpiece. Due to this uneven temperature change, rise in both previously laid layer and the newly deposited layer. These stresses affect dimensions and shape of final workpieces. Materials can exhibit various distortions, including transverse or longitudinal shrinkage, bending, and angular distortion. It is thought that deterioration can be prevented by changing the IPs of the samples. Because IP structures change the number

of connections (Number of points) and shapes between layers in the samples. It is known that this situation will provide a higher mechanical strength to the material [59]. For this reason, it is thought that internal stresses can be minimized in samples produced by using the optimum IP and LT [60].

Microscopic images for hexagon, triangle and line patterns are given in Fig. 10. These images show surface conditions according to different infill pattern and height of layer characteristics. Orientation lines and small voids between layers were observed on the surfaces of the examined materials. It is thought that these surface conditions occur depending on the production characteristics in line with the independent variables used, as mentioned before.

4. CONCLUSION

In this research investigation, mechanical features of PLA, ABS and ePA-CF materials produced with FDM method in different IP and LT were experimentally investigated. It was determined that workpiece with the best mechanical features among the samples produced was the one produced with ePA-CF in a LT of 0.15 mm and a hexagon pattern. The best mechanical properties for the PLA sample were determined with a LT of 0.15 mm and a hexagon pattern. It was seen that the worst mechanical features were given in LT of 0.35 mm and triangle pattern. It was found that the ABS sample exhibited the best mechanical properties with a LT of 0.15mm and a triangle pattern. Conversely, the worst mechanical properties were observed with a LT of 0.35 mm and triangle pattern. For the ePA- CF material, the best mechanical properties were observed in samples manufactured with LT of 0.15 mm and a hexagon pattern. The worst mechanical properties were detected in samples with LT of 0.35 mm and line pattern. It was revealed that tensile, YS and elongation values decrease as a result of increasing LT. It was stated that the air voids between the layers occurred the most in the PLA sample and the least in the ePA-CF sample. The fracture surfaces of samples produced with PLA were found to be smooth with distinct layer lines. It was understood that this was due to insufficient bonding between layers. It was found that the fracture surfaces of workpieces manufactured with ABS were rough and layer lines were less distinct than the PLA sample. Since ABS samples had an anisotropic structure, it was stated that the fracture occurs along the direction in which the layers were stacked. Observations revealed that the carbon fiber reinforcement material was prominently visible on the fracture surfaces of samples produced from ePA-CF material. Fractures were found to occur in a more fibrous structure. It was established that correctly matching printing parameters with the material used was crucial. It was found that reducing the number and size of voids within the internal structure of samples and altering the base material with the addition of different ingredients such as CF, further improves mechanical properties.

REFERENCES

1. Maheshwari, S., Alam, Z., Singh, S.S., 2024, *Investigating the large strain compression properties of PLA parts manufactured by FDM using experiments and constitutive modeling*, Rapid Prototyping Journal, 30(3), pp. 555-570.

2. Thompson, M. K., Moroni, G., Vaneker, T., Fadel, G., Campbell, R. I., Gibson, I., Martina, F., 2016, *Design for Additive Manufacturing: Trends, opportunities, considerations, and constraints.* CIRP annals, 65(2), pp. 737-760.
3. Bandyopadhyay A., Heer, B., 2018, *Additive manufacturing of multi-material structures*, Materials Science and Engineering: R: Reports, 129, pp. 1-16.
4. Oropallo, W., Piegl, L.A., 2016, *Ten challenges in 3D printing*, Engineering with Computers, 32, pp. 135–148.
5. Wu, F., Lian, H., Pei, G., Guo, B., Wang, Z., 2023, *Design and optimization of the variable-density lattice structure based on load paths*, Facta Universitatis, Series: Mechanical Engineering, 21(2), pp. 273-292.
6. Moreno, N.D., Molina, S.I., 2020, *Large-format fused deposition additive manufacturing: a review*, Rapid Prototyping Journal, 26(5), pp. 793-799.
7. Ngo, T.D., Kashani, A., Imbalzano, G., Nguyen, K.T., Hui, D., 2018, *Additive manufacturing (3D printing): A review of materials, methods, applications and challenges*, Composites Part B: Engineering, 143, pp. 172-196.
8. Milićević, I., Popović, M., Dučić, N., Vujičić, V., Stepanić, P., Marinković, D., Ćojbašić, Ž., 2022, *Improving the mechanical characteristics of the 3D printing objects using hybrid machine learning approach*, Facta Universitatis, Series: Mechanical Engineering, 10.22190/FUME220429036M.
9. Gibson, I., Rosen, D., Stucker, B., Khorasani, M., 2021, *Additive manufacturing Technologies*, Springer, Cham: Switzerland.
10. Li, S., 2021, *The Quest for Product Safety in the Context of 3D Printing: A Law and Economics Analysis*, PhD Thesis, Universities of Bologna, Italy.
11. Bayraktar, Ş., Alparslan, C., 2023, *Comparison of the SLM, SLS, and DLMS techniques in additive manufacture of AlSi10Mg alloys*, pp. 231-253, *In Innovation and Sustainable Manufacturing*, Woodhead Publishing.
12. Chu, M.Q., Wang, L., Ding, H.Y., Sun, Z.G., 2015, *Additive manufacturing for aerospace application*, Applied Mechanics and Materials, 798, pp. 457-461.
13. Cano-Vicent, A., Tambuwala, M.M., Hassan, S.S., Barh, D., Aljabali, A.A., Birkett, M., Serrano-Aroca, Á., 2021, *Fused deposition modelling: Current status, methodology, applications and future prospects*, Additive manufacturing, 47, pp. 102378.
14. Singh, P., Singari, R.M., Mishra, R.S., 2024, *Enhanced mechanical properties of MWCNT reinforced ABS nanocomposites fabricated through additive manufacturing process*, Polymers for Advanced Technologies, 35(2), e6308.
15. Senatov, F.S., Niaza, K.V., Stepashkin, A.A., Kaloshkin, S.D., 2016, *Low-cycle fatigue behavior of 3d-printed PLA-based porous scaffolds*, Composites Part B: Engineering, 97, pp. 193-200.
16. Daminabo, S.C., Goel, S., Grammatikos, S.A., Nezhad, H.Y., Thakur, V.K., 2020, *Fused deposition modeling-based additive manufacturing (3D printing): techniques for polymer material systems*, Materials today chemistry, 16, 100248.
17. Dave, H.K., Davim, J.P., 2021, *Fused deposition modeling based 3D printing*, Springer International Publishing, Cham: Switzerland.
18. Song, X., He, W., Chen, P., Wei, Q., Wen, J., Xiao, G., 2021, *Fused deposition modeling of poly (lactic acid)/almond shell composite filaments*, Polymer Composites, 42(2), pp. 899-913.
19. Proikakis, C.S., Tarantili, P.A., Andreopoulos, A.G., 2006, *The role of Polymer/Drug interactions on the Sustained Release from Poly (D, L-Lactic acid) Tablets*, European Polymer Journal, 42(12), pp. 3269-3276.
20. Athanasiou, K.A., Niederauer, G.G., Agrawal, C.M., 1996, *Sterilization, Toxicity, Biocompatibility and Clinical Applications of Polylactic Acid/Polyglycolic Acid Copolymers*, Biomaterials, 17(2), pp. 93-102.
21. Dakshinamurthy, D., Gupta, S., 2018, *A study on the influence of process parameters on the viscoelastic properties of ABS components manufactured by FDM process*. Journal of The Institution of Engineers (India): Series C, 99, pp. 133-138.
22. Shashikumar, S., Sreekanth, M. S., 2024, *Investigation on mechanical properties of polyamide 6 and carbon fiber reinforced composite manufactured by fused deposition modeling technique*, Journal of Thermoplastic Composite Materials, 37(5), pp. 1730-1747.
23. Yu, W., Sun, L., Li, M., Li, M., Lei, W., Wei, C., 2023, *FDM 3D printing and properties of PBS/PLA blends*, Polymers, 15(21), 4305.
24. Sedlacek, F., & Lašová, V., 2018, *Additive manufacturing of PA6 with short carbon fibre reinforcement using fused deposition modelling*, Materials Science Forum, 928, pp. 26-31.
25. Farashi, S., Vafaee, F., 2022, *Effect of extruder temperature and printing speed on the tensile strength of fused deposition modeling (FDM) 3D printed samples: A meta-analysis study*, International Journal on Interactive Design and Manufacturing, 16(1), pp. 305-316.

26. Bochnia, J., Blasiak, M., Kozior, T., 2021, *A Comparative Study of the Mechanical Properties of FDM 3D Prints Made of PLA and Carbon Fiber-Reinforced PLA for Thin-Walled Applications*, Materials, 14 (22), 7062.
27. Chalgham, A., Ehrmann, A., Wickenkamp, I., 2021, *Mechanical properties of FDM printed PLA parts before and after thermal treatment*, Polymers, 13(8), 1239.
28. Samykano, M., Selvamani, S.K., Kadirgama, K., 2019, *Mechanical property of FDM printed ABS: Influence of printing parameters*, The International Journal of Advanced Manufacturing Technology, 102(9), pp. 2779-2796.
29. Khabia, S., Jain, K.K., 2020, *Comparison of mechanical properties of components 3D printed from different brand ABS filament on different FDM printers*, Material Today: Proceedings, 26, pp. 2907-2914.
30. Pazhamannil, R.V., Govindan, P., Edacherian, A., Hadidi, H.M., 2024, *Impact of process parameters and heat treatment on fused filament fabricated PLA and PLA-CF.*, International Journal on Interactive Design and Manufacturing, 18, pp. 2199-2213.
31. Reverte, J.M., Caminero, M.Á., Chacón, J.M., 2020, *Mechanical and geometric performance of PLA-based polymer composites processed by the fused filament fabrication additive manufacturing technique*, Materials, 13(8), 1924.
32. Dhinesh, S.K., Arun, P.S., Senthil, K.K., Megalingam, A., 2021, *Study on flexural and tensile behavior of PLA, ABS and PLA-ABS materials*, Material Today: Proceedings, 45, pp. 1175-1180.
33. www.dukkan.3d3teknoloji.com/filament-ve-recine-pmk3 (last access: 10.03.2024)
34. www. esun3d.com (last access: 10.03.2024)
35. www.flashforge.com/product-detail/flashforge-creator-3-fdm-3d-printer (last access: 10.03.2024)
36. Laureto, J.J., Pearce, J.M., 2018, *Anisotropic mechanical property variance between ASTM D638-14 type i and type iv fused filament fabricated specimens,* Polymer Testing, 68, pp. 294-301.
37. Anand Kumar, S., Shivraj Narayan, Y., 2019, *Tensile testing and evaluation of 3D-printed PLA specimens as per ASTM D638 type IV standard,* In Innovative Design, Analysis and Development Practices in Aerospace and Automotive Engineering (I-DAD), 2, pp. 79-95.
38. Pejkowski, Ł., Seyda, J., Nowicki, K., Mrozik, D., 2023, *Mechanical performance of non-reinforced, carbon fiber reinforced and glass bubbles reinforced 3D printed PA12 polyamide,* Polymer Testing, 118, 107891.
39. Zhu, Z., He, H., Xue, B., Zhan, Z., Wang, G., Chen, M., 2018, *Morphology, thermal, mechanical properties and rheological behavior of biodegradable poly (butylene succinate)/poly (lactic acid) in-situ submicrofibrillar composites,* Materials, 11(12), 2422.
40. Qian, K., Qian, X., Chen, Y., Zhou, M., 2018, *Poly (lactic acid)–thermoplastic poly (ether) urethane composites synergistically reinforced and toughened with short carbon fibers for three‐dimensional printing*, Journal of Applied Polymer Science, 135 (29), 46483.
41. Nomani, J., Wilson, D., Paulino, M., Mohammed, M.I., 2020, *Effect of layer thickness and cross-section geometry on the tensile and compression properties of 3D printed ABS,* Materials Today Communications, 22, 100626.
42. Xu, Z., Fostervold, R., Razavi, N., 2021, *Thickness effect on the mechanical behavior of PLA specimens fabricated via Fused Deposition Modeling,* Procedia Structural Integrity, 33, pp. 571-577.
43. Pinto, V.C., Ramos, T., Alves, A. S. F., Xavier, J., Tavares, P. J., Moreira, P.M.G.P., Guedes, R.M., 2017, *Dispersion and failure analysis of PLA, PLA/GNP and PLA/CNT-COOH biodegradable nanocomposites by SEM and DIC inspection*, Engineering failure analysis, 71, pp. 63-71.
44. Naveed, N., 2021, *Investigating the material properties and microstructural changes of fused filament fabricated PLA and tough-PLA parts*, Polymers, 13(9), 1487.
45. Rajpurohit, S.R., Dave, H.K., 2021, *Impact strength of 3D printed PLA using open source FFF-based 3D printer*, Progress in Additive Manufacturing, 6(1), pp. 119-131.
46. Rahmatabadi, D., Ghasemi, I., Baniassadi, M., Abrinia, K., Baghani, M., 2022, *3D printing of PLA-TPU with different component ratios: Fracture toughness, mechanical properties, and morphology*, Journal of Materials Research and Technology, 21, pp. 3970-3981.
47. Vicente, C.M., Martins, T.S., Leite, M., Ribeiro, A., Reis, L., 2020, *Influence of fused deposition modeling parameters on the mechanical properties of ABS parts,* Polymers for Advanced Technologies, 31(3), pp. 501-507.
48. Azadi, M., Dadashi, A., Dezianian, S., Kianifar, M., Torkaman, S., Chiyani, M., 2021, *High-cycle bending fatigue properties of additive-manufactured ABS and PLA polymers fabricated by fused deposition modeling 3D-printing*, Forces in Mechanics, 3, 100016.
49. Torrado Perez, A.R., Roberson, D.A., Wicker, R.B., 2014, *Fracture surface analysis of 3D-printed tensile specimens of novel ABS-based materials,* Journal of Failure Analysis and Prevention, 14, pp. 343-353.

50. Vidakis, N., Petousis, M., Velidakis, E., Liebscher, M., Mechtcherine, V., Tzounis, L., 2020, *On the strain rate sensitivity of fused filament fabrication (Fff) processed pla, abs, petg, pa6, and pp thermoplastic polymers*, Polymers, 12(12), 2924.
51. Nabavi-Kivi, A., Ayatollahi, M.R., Razavi, N., 2023, *Investigating the effect of raster orientation on fracture behavior of 3D-printed ABS specimens under tension-tear loading*, European Journal of Mechanics-A/Solids, 99, 104944.
52. Tutar, M., 2022, *A Comparative Evaluation of the Effects of Manufacturing Parameters on Mechanical Properties of Additively Manufactured PA and CF-Reinforced PA Materials*, Polymers, 15(1), 38.
53. Russias, J., Saiz, E., Nalla, R.K., Gryn, K., Ritchie, R.O., Tomsia, A.P., 2006, *Fabrication and mechanical properties of PLA/HA composites: a study of in vitro degradation*, Materials Science and Engineering: C, 26(8), pp. 1289-1295.
54. Bax, B., Müssig, J., 2008, *Impact and tensile properties of PLA/Cordenka and PLA/flax composites*, Composites Science and Technology, 68(7-8), pp. 1601-1607.
55. Arunkumar, N., Sathishkumar, N., Sanmugapriya, S.S., Selvam, R., 2021, *Study on PLA and PA thermoplastic polymers reinforced with carbon additives by 3D printing process*, Materials Today: Proceedings, 46, pp. 8871-8879.
56. Blok, L.G., Longana, M.L., Yu, H., Woods, B.K., 2018, *An investigation into 3D printing of fibre reinforced thermoplastic composites*, Additive Manufacturing, 22, pp. 176-186.
57. Brenken, B., Barocio, E., Favaloro, A., Kunc, V., Pipes, R.B., 2018, *Fused filament fabrication of fiber-reinforced polymers: A review*, Additive Manufacturing, 21, pp. 1-16.
58. Li, H., Wang, T., Li, Q., Yu, Z., Wang, N., 2018, *A quantitative investigation of distortion of polylactic acid/PLA) part in FDM from the point of interface residual stress*, The International Journal of Advanced Manufacturing Technology, 94, pp. 381-395.
59. Baldi, A, Considine, M., Quinn, S., Balandraud, X., 2018, *Residual Stress, thermomechanics & infrared imaging, hybrid techniques and inverse problems*, Proceedings of the 2017 Annual Conference on Experimental and Applied Mechanics. Springer.
60. Zhang, W., Wu, A.S., Sun, J., Quan, Z., Gu, B., Sun, B., Chou, T.W., 2017, *Characterization of residual stress and deformation in additively manufactured ABS polymer and composite specimens*, Composites Science and Technology, 150, pp. 102-110.